

# The Taylor instability and the Hall effect in protoneutron stars

G. Rüdiger<sup>1,\*</sup>, M. Schultz<sup>1</sup>, M. Mond<sup>2</sup>, and D.A. Shalybkov<sup>3</sup>

<sup>1</sup> Astrophysikalisches Institut Potsdam, An der Sternwarte 16, D-14482 Potsdam, Germany

<sup>2</sup> Department of Mechanical Engineering, Ben-Gurion University of the Negev, P.O. Box 653, Beer-Sheva 84105, Israel

<sup>3</sup> A.F. Ioffe Institute for Physics and Technology, 194021, St. Petersburg, Russia

Received 2008, accepted 2008

Published online 2008

**Key words** neutron stars – instabilities – magnetohydrodynamics – magnetic fields – plasmas

Collapse calculations indicate that the hot newly born protoneutron stars (PNS) rotate differentially so that strong toroidal magnetic field components should exist in the outer crust where also the Hall effect appears to be important when the Hall parameter  $\hat{\beta} = \omega_B \tau$  is of order unity. The amplitudes of the induced toroidal magnetic fields are limited from above by the Taylor instability. An important characteristic of the Hall effect is its distinct dependence on the *sign* of the magnetic field. We find for fast rotation that positive (negative) Hall parameters essentially reduce (increase) the stability domain. It is thus concluded that the toroidal field belts in PNS induced by their differential rotation should have different amplitudes in both hemispheres which later are frozen in. Due to the effect of magnetic suppression of the heat conductivity also the brightness of the two hemispheres should be different. As a possible example for our scenario the isolated neutron star RBS 1223 is considered which has been found to exhibit different X-ray brightness at both hemispheres.

© 2008 WILEY-VCH Verlag GmbH & Co. KGaA, Weinheim

## 1 Introduction

Progenitors of neutron stars are high-mass stars with more than eight solar masses that develop a degenerate iron core. If the core mass approaches the Chandrasekhar limit it becomes gravitationally unstable and implodes. The collapse comes to a temporary end if nuclear densities are reached. At that stage the rebounding inner core drives a shock wave into the outer core, a mechanism that is currently believed to be responsible for the appearance of supernova.

If the core of the supergiant rotates already rapidly the neutron star will be born as a fast rotator with an angular velocity near the break-off value, i.e. 1 kHz. This value exceeds the rotation rate of the fastest young pulsars known by one order of magnitude so that the question arises how a critically rotating protoneutron star (PNS) spins down. One possibility is the angular momentum loss by gravitational wave emission via unstable r-modes (Friedman & Schutz 1978; Andersson 1998; Stergioulas & Font 2001; Lindblom, Tohline & Vallisneri 2001). As the viscous damping of the r-modes is smallest at temperatures around  $10^9$  K, this instability works best as long as the neutron star remains hot. Up to 90% of the rotational energy can be removed in that way from the newly formed neutron star within hours. Other possibilities involve angular momentum transport due to non-axisymmetric instabilities also connected with gravitational waves.

Following Burrows (1987), entropy-driven convection may play an essential role in the neutrino-mediated supernova explosion scenario since it enhances the neutrino lu-

minosities in the post-collapse stage. Such a convection might be important with regard to a standard-dynamo action in PNS (Thompson & Duncan 1993). If, on the other hand, additionally differential rotation exists in the turbulent domain, then an  $\alpha\Omega$ -dynamo can work producing strong toroidal magnetic fields (Bonanno et al. 2003, 2006). Indeed, hydrodynamic simulations of rotational supernova core collapse have shown that even a nearly rigidly rotating initial core results in a strongly differentially rotating post-collapse neutron star (Mönchmeyer & Müller 1989; Janka & Mönchmeyer 1989; Dimmelmeier, Font & Müller 2002; Kotake et al. 2004; Ardeljan et al. 2005; Burrows et al. 2007). Any nonhomologous collapse creates necessarily some degree of differential rotation if angular momentum is conserved locally during collapse. The models reveal a strong differential rotation in the azimuthally averaged angular velocity (Ott et al. 2005). Differential rotation may furthermore be generated by r-modes via nonlinear effects (Rezzolla, Lamb & Shapiro 2000) or simply by accreting falling-back material (Watts & Andersson 2002).

### 1.1 Differential rotation and magnetic fields

In the presence of a poloidal field  $B_R$ , differential rotation with a shear  $q$  produces a toroidal field component by induction. The ratio of the resulting field to the original one can simply be estimated as

$$\epsilon \equiv \frac{B_\phi}{B_R} \simeq q\Omega\tau \quad \text{if } \epsilon < \text{Rm}, \quad (1)$$

with Rm as the magnetic Reynolds number of the differential rotation. For high Rm the differential rotation may induce strong toroidal fields. Also flux compression will play

\* Corresponding author: gruediger@aip.de

an important role in amplification of both poloidal fields and toroidal fields (Burrows et al. 2007). However, the resulting magnetic field transports angular momentum outwards and feedbacks the differential rotation. The timescale of this backreaction is

$$\tau = \frac{\mu_0 \rho q \Omega L^2}{B_R B_\phi} = \frac{\mu_0 \rho q \Omega L^2}{\epsilon B_R^2}. \quad (2)$$

With  $\epsilon \simeq q \Omega \tau$  one finds

$$\tau \simeq \frac{\sqrt{\mu_0 \rho} L}{B_R}, \quad (3)$$

i.e. the Alfvén travel time of 1...10 s (Shapiro 2000). Hence, after (1)  $\epsilon \simeq 100 \dots 1000$ . Typical values of the neutron stars have been used:  $\rho \simeq 10^{13}$  g/cm<sup>3</sup>,  $\Omega \simeq 100$  s<sup>-1</sup>,  $L \simeq 10^5$  cm (the crust thickness) and  $B_r \simeq 10^{12}$  G. Note that for  $\epsilon \simeq 1000$  the differential rotation is immediately destroyed. We find  $\epsilon < 1000$  (i.e.  $B_{\text{tor}} < 10^{15}$  G) as a necessary condition for the existence of differential rotation over several rotation periods. This value is a rather small value insofar as

$$\epsilon_{\text{max}} \simeq \text{Rm} = \frac{\Omega L^2}{\eta} \simeq \frac{10^{12} \text{ cm}^2/\text{s}}{\eta}, \quad (4)$$

so that already for  $\eta < 10^9$  cm<sup>2</sup>/s the critical  $\epsilon$  is exceeded. The microscopic value is only  $\eta \simeq 10^{-6}$  cm<sup>2</sup>/s. It is obvious that with such a small microscopic value a differential rotation cannot survive. It is an open question whether such high values of  $\eta$  can be reached in neutron stars (see Naso et al. 2007).

The diffusion time  $L^2/\eta$  for  $\eta \simeq 10^9$  cm<sup>2</sup>/s is also 10 s which, however, would also be the decay time of the differential rotation for magnetic Prandtl number  $\text{Pm} \geq 1$ . With such high values of viscosity a prescribed differential rotation cannot exist longer than a few rotations.

In the present paper we assume that differential rotation exists for at least 10 s ( $\simeq 100$  rotations). During this time r-modes are excited producing gravitational waves. The viscosity must thus be  $\lesssim 10^9$  cm<sup>2</sup>/s. This value corresponds to the expression  $\nu \simeq \alpha L^2 \Omega$  with  $\alpha \simeq 10^{-3}$  which is known from the accretion theory (due to small-scale MRI). As the microscopic magnetic Prandtl number  $\text{Pm}$  is very large for neutron stars we also continue with a high magnetic Prandtl number for the unstable PNS crust matter, say  $\text{Pm} \simeq 100$  so that  $\eta \simeq 10^7$  cm<sup>2</sup>/s. In that case the magnetic diffusion time exceeds the viscous time by a factor of 100 and the magnetic Reynolds number is of order  $10^5$ . The differential rotation would thus generate huge toroidal fields with  $\epsilon \simeq 10^5$  which, however, would destroy the differential rotation.

Therefore, in the present paper the stability of strong toroidal magnetic fields against nonaxisymmetric perturbations is probed in order to find their real upper limits. We are thus considering the Tayler instability under the influence of differential rotation and for high magnetic Prandtl numbers. The toroidal field is assumed to dominate the poloidal field ( $\epsilon > 1$ ) so that stability under only toroidal field is considered. To that end, as will be shown in the next section, also the influence of the Hall effect in neutron stars must be taken into account.

## 1.2 Magnetic fields and Hall effect in neutron stars

Neutron stars have the strongest magnetic fields found in the Universe, with fields exceeding  $10^{13}$  G for young ( $\sim 10^7$  yr) radio and X-ray pulsars, and a still appreciable  $10^8$ – $10^{10}$  G for much older ( $\sim 10^{10}$  yr) millisecond pulsars. This correlation between field strength and age suggests that these very different strengths are due to the field decaying in time rather than to differences between different neutron stars.

Jones (1988) and Goldreich & Reisenegger (1992) have proposed that correlation between the magnetic field of the neutron star and its age is due to the Hall drift. Since the Hall effect enters the evolution equation for  $\mathbf{B}$  as a quadratic non-linearity, it necessarily leads to a timescale inversely proportional to  $|\mathbf{B}|$ . The Hall effect is therefore attractive for explaining the variations in the decay rates (for  $B \sim 10^{13}$  G the field should evolve on a  $10^7$  year timescale while if  $B \sim 10^{10}$  G it should evolve on a  $10^{10}$  year timescale).

There is a bulk of literature about the existence of the Hall effect in neutron stars. The main findings may be summarized as follows. The Hall effect strongly depends on the magnetic field amplitude and the temperature of the neutron star. In the presence of strong magnetic fields the magnetic diffusivity is anisotropic and is given by a tensor whose components along the magnetic field are  $\eta_{\parallel}$ , the components perpendicular to the magnetic field are  $\eta_{\perp}$ , and off-diagonal Hall component  $\eta_{\text{H}}$ . For more details concerning the generalized Ohm's law in multi-component plasma we refer to the papers Yakovlev & Shalybkov (1991) and Shalybkov & Urpin (1995).

With Hall effect included the magnetic induction equation takes the general form

$$\frac{\partial \mathbf{B}}{\partial t} - \eta \Delta \mathbf{B} = \text{curl}(\mathbf{u} \times \mathbf{B} - \beta \text{curl} \mathbf{B} \times \mathbf{B}) \quad (5)$$

with  $\eta \equiv \eta_{\perp}$  and  $\beta = c/4\pi e n_e$ , where  $n_e$  is the electrons' number density. In addition, it is useful to define the Hall magnetic diffusivity as  $\eta_{\text{H}} \equiv \beta B$ . The Hall effect becomes important if  $\hat{\beta} > 1$ , where

$$\hat{\beta} = \frac{\eta_{\text{H}}}{\eta_{\perp}}. \quad (6)$$

For magnetic fields smaller than some critical value,  $B_{\text{cr}}$ ,  $\eta_{\perp} = \eta_{\parallel} = \eta_0$  where  $\eta_0$  is the magnetic diffusivity without an applied magnetic field. If  $B > B_{\text{cr}}$  then  $\eta_{\perp}$  increases as  $B^2$  for increasing magnetic field. The Hall magnetic diffusivity, on the other hand, is proportional to the magnetic field value. As a result, the Hall effect can be important only in some vicinity of the  $B_{\text{cr}}$ .

The critical magnetic field can vary significantly within the neutron star envelopes depending on chemical composition, temperature and density. According to Potekhin (1999) the critical magnetic field is  $\sim 10^{12}$  G for iron composition with temperature  $10^8$  K and density  $10^{11}$  g/cm<sup>3</sup>. Detailed calculations of the electrical conductivity in pure neutron star crusts (Cumming et al. 2004) indicate that the Hall time scale under such parameters is indeed shorter than the

Ohmic decay time, which means that  $\hat{\beta} > 1$ . One finds<sup>1</sup> that for iron ( $Z=26$ ,  $A=56$ ) with  $\rho = 10^{13}$  g/cm<sup>3</sup> the  $\hat{\beta}$  varies from  $10^{-3}B_{12}$  for  $T = 10^{10}$  K to  $3B_{12}$  for  $10^8$  K. Note, however, that for the same plasma the Hall parameter  $\hat{\beta}$  reaches a maximal value of  $\sim 10$  for  $B \sim 10^{13}$  G and decreases for higher magnetic field values.

Hence, it makes sense to ask for the consequences of the Hall term for young neutron stars with fields of  $B_{12} \gg 1$  which can be imagined – and this is the point here – as toroidal field due to the induction of a differential rotation. Important for us is only the assumption that the (early) phase of the existence of differential rotation in the crust of the PNS is accompanied by  $\hat{\beta}$  of order unity for the resulting toroidal fields. Obviously,  $\hat{\beta}$  linearly depends on the magnetic amplitude so that we can write

$$\hat{\beta} = \beta_0 \sqrt{\text{Pm}} \text{Ha} = \beta_0 S, \quad (7)$$

with  $S$  as the Lundquist number (see below). The parameter  $\beta_0$  does not depend on the magnetic field<sup>2</sup>.

To estimate the magnetic Prandtl number we should also use  $\eta_{\perp}$  instead of  $\eta_0$ . We will have smaller magnetic Prandtl numbers for the parameters where the Hall effect is important. Nevertheless, it is easy to estimate that the magnetic Prandtl number can be much larger than 1 for the typical neutron star envelopes parameters.

## 2 Taylor instability

Differential rotation leads to an increase of the toroidal component of the magnetic field by winding up the poloidal field lines. The ratio of both components is given by the magnetic Reynolds number of the differential rotation which is very large also for PNS due to their small values of the magnetic diffusivity  $\eta$ . The same is true for the microscopic magnetic Prandtl number ( $\nu \simeq 10$  cm<sup>2</sup>/s,  $\eta \simeq 10^{-6}$  cm<sup>2</sup>/s).

Too strong toroidal fields, however, become unstable against the Tayler instability. Tayler (1961, 1973) and Vankurov (1972) considered the stability of nonaxisymmetric disturbances and showed that for an ideal fluid the necessary and sufficient condition for stability is

$$\frac{d}{dR}(RB_{\phi}^2) < 0. \quad (8)$$

An almost uniform field would therefore be stable against axisymmetric perturbations but unstable against nonaxisymmetric perturbations (with  $m = 1$  being the most unstable mode). Differentially rotating PNS might be susceptible to that kink-type instability that in turn may limit their magnetic field amplitude.

Criterion (8) cannot be applied directly to fields under the influence of differential rotation. In a first step to understand the complicated interaction of toroidal magnetic fields and differential rotation we have studied a Taylor-Couette container with two corotating cylinders where the radial rotation law is hydrodynamically stable. An electric current

is flowing parallel to the rotation axis through the conducting fluid, thus producing a nearly uniform toroidal magnetic field. It becomes unstable against nonaxisymmetric perturbations for non rotating cylinders but only for a rather strong magnetic field. If measured in terms of Hartmann numbers,

$$\text{Ha} = \frac{B_0 R_0}{\sqrt{\mu_0 \rho \nu \eta}}, \quad (9)$$

with  $R_0 = \sqrt{(R_{\text{out}} - R_{\text{in}})R_{\text{out}}}$ , this is at about  $\text{Ha} = 150$  (see Fig. 1). In case of rotating cylinders without magnetic field the rotation law may be so flat that it is hydrodynamically stable. With magnetic fields it becomes always unstable (Rüdiger et al. 2007). One finds that differential rotation is strongly *destabilizing for large magnetic Prandtl numbers* which are characteristic for the PNS matter. One can thus expect that the toroidal magnetic fields induced by the differential rotation of PNS are limited by the described current-induced instability.

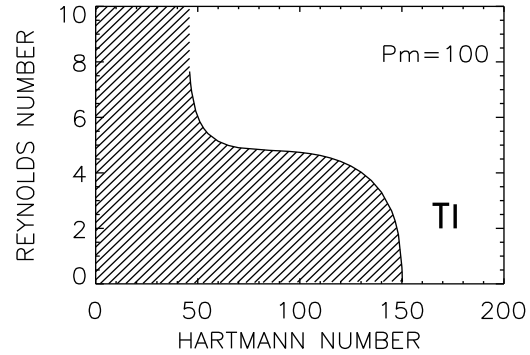


**Fig. 1** The stability domain (hatched) for outer cylinder rotating with 50% of the inner cylinder ( $\mu_{\Omega} = 0.5$ ), the magnetic field is almost uniform ( $\mu_B = 1$ ), the perturbations are nonaxisymmetric ( $m = 1$ ). Note the destabilizing action of high magnetic Prandtl numbers (here  $\text{Pm} = 100$ ).

In the present paper the stability problem for strong toroidal magnetic fields under the influence of differential rotation and the Hall effect is considered. We shall see that in this case even the sign of the toroidal field (with respect to the global rotation) will play an important role.

## 3 The basic equations

The basic state in the cylindrical system is  $U_R = U_z = B_R = B_z = 0$  and

$$B_{\phi} = AR + \frac{B}{R}, \quad U_{\phi} = R\Omega = aR + \frac{b}{R}, \quad (10)$$

where  $a$ ,  $b$ ,  $A$  and  $B$  are constant values defined by

$$a = \Omega_{\text{in}} \frac{\mu_{\Omega} - \hat{\eta}^2}{1 - \hat{\eta}^2}, \quad b = \Omega_{\text{in}} R_{\text{in}}^2 \frac{1 - \mu_{\Omega}}{1 - \hat{\eta}^2},$$

$$A = \frac{B_{\text{in}} \hat{\eta} (\mu_B - \hat{\eta})}{R_{\text{in}} (1 - \hat{\eta}^2)}, \quad B = B_{\text{in}} R_{\text{in}} \frac{1 - \mu_B \hat{\eta}}{1 - \hat{\eta}^2}. \quad (11)$$

<sup>1</sup> see <http://www.ioffe.rssi.ru/astro/conduct/>

<sup>2</sup> Other possible notations for  $\hat{\beta}$  are  $\hat{\beta} = \text{Rb} = a_e = \omega_B \tau$

Here is

$$\hat{\eta} = \frac{R_{\text{in}}}{R_{\text{out}}}, \quad \mu_{\Omega} = \frac{\Omega_{\text{out}}}{\Omega_{\text{in}}}, \quad \mu_B = \frac{B_{\text{out}}}{B_{\text{in}}}, \quad (12)$$

with  $R_{\text{in}}$  and  $R_{\text{out}}$  as the radii,  $\Omega_{\text{in}}$  and  $\Omega_{\text{out}}$  the angular velocities, and  $B_{\text{in}}$  and  $B_{\text{out}}$  as the azimuthal magnetic fields of the inner and the outer cylinders. The possible magnetic field solutions which do not decay are plotted in Fig. 2.

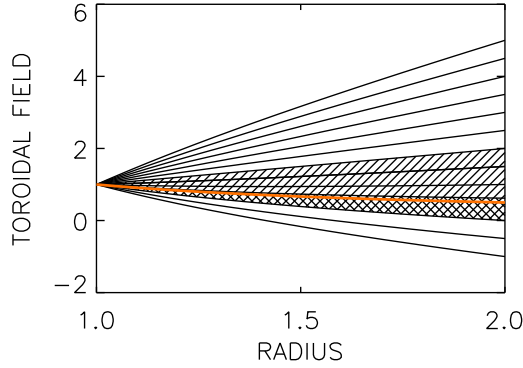


**Fig. 2** The possible radial profiles of the toroidal magnetic field between the two cylinders. The value of the intersection of each of the profiles with the right vertical axis is the corresponding  $\mu_B$ -value. The profiles in the hatched domain are stable against axisymmetric perturbations while the cross-hatched area is also stable against nonaxisymmetric perturbations. The current-free solution  $B_{\phi} \propto 1/R$  is given by the red line.

We are interested now in the linear stability of the background state (10). In that case, the perturbed quantities of the system are given by

$$u_R, R\Omega + u_{\phi}, u_z, b_R, B_{\phi} + b_{\phi}, b_z. \quad (13)$$

As usual, the perturbations are developed in normal modes of the form

$$F = F(R)\exp(i(kz + m\phi + \omega t)). \quad (14)$$

Terms of the form (13) and (14) are inserted now into the the induction equation (5) with the Hall effect included and linearized about the background state. The result is:

$$\frac{\partial \mathbf{B}}{\partial t} - \eta \Delta \mathbf{B} = \mathbf{E} - \beta \mathbf{H} \quad (15)$$

with

$$E_R = \frac{1}{R} (im u_R B_{\phi} - im R \Omega b_R), \quad (16)$$

$$E_{\phi} = -\frac{dB_{\phi}}{dR} u_R + \Omega R \frac{db_R}{dR} + \frac{d\Omega}{dR} R b_R - B_{\phi} \frac{du_R}{dR} - B_{\phi} i k u_z + \Omega b_R + i k \Omega R b_z, \quad (17)$$

$$E_z = \frac{1}{R} (im u_z B_{\phi} - im R \Omega b_z) \quad (18)$$

and the Hall terms

$$H_R = \frac{1}{R^2} \left( -\frac{dB_{\phi}}{dR} i k R^2 b_R + B_{\phi} k m R b_{\phi} - B_{\phi} i k R b_R - B_{\phi} m^2 b_z \right), \quad (19)$$

$$H_{\phi} = \frac{1}{R^2} \left( -\frac{dB_{\phi}}{dR} i m R b_z - B_{\phi} i m R \frac{db_z}{dR} - 2B_{\phi} i k R b_{\phi} - B_{\phi} k m R b_R + B_{\phi} i m b_z \right), \quad (20)$$

$$H_z = \frac{1}{R^2} \left( \frac{dB_{\phi}}{dR} R^2 b_R + \frac{dB_{\phi}}{dR} R^2 \frac{db_R}{dR} + \frac{dB_{\phi}}{dR} i m R b_{\phi} + 2 \frac{dB_{\phi}}{dR} R b_R + B_{\phi} i m R \frac{db_{\phi}}{dR} + B_{\phi} R \frac{\partial b_R}{\partial R} + 2B_{\phi} i m b_{\phi} + B_{\phi} m^2 b_R \right). \quad (21)$$

The dimensionless numbers of the problem are the magnetic Prandtl number (Pm), the Hartmann number (Ha) and the Reynolds number (Re), i.e.

$$\text{Pm} = \frac{\nu}{\eta}, \quad \text{Ha} = \frac{B_{\text{in}} R_0}{\sqrt{\mu_0 \rho \nu \eta}}, \quad \text{Re} = \frac{\Omega_{\text{in}} R_0^2}{\nu}, \quad (22)$$

where  $R_0 = (R_{\text{in}}(R_{\text{out}} - R_{\text{in}}))^{1/2}$  is the characteristic length scale,  $\nu$  the kinematic viscosity and  $\eta$  the magnetic diffusivity. The magnetic Reynolds number is  $\text{Rm} = \text{Pm} \text{Re}$  and the Lundquist number is  $S = \sqrt{\text{Pm}} \text{Ha}$ .

We use  $R_0$  as a unit of length and  $R_0^{-1}$  as a unit of the wave number,  $\eta/R_0$  as a unit of the perturbed velocity,  $\Omega_{\text{in}}$  as a unit of angular velocity and  $\omega$ , and  $B_{\text{in}}$  as a unit of magnetic fields (basic and disturbed).

In normalized quantities eq. (15) may be cast in the following form:

$$i\omega \text{Rm} \mathbf{b} = D(\mathbf{b}) + \hat{\mathbf{E}} - \hat{\beta} \mathbf{H} \quad (23)$$

with

$$\hat{E}_R = \frac{1}{R} \left( i m \hat{B} u_R - i m R \text{Rm} \hat{\Omega} b_R \right), \quad (24)$$

$$\hat{E}_{\phi} = -\hat{B}' u_R - i k \hat{B} u_z - \hat{B} \frac{du_R}{dR} + \text{Rm} \left( R \hat{\Omega} \frac{db_R}{dR} + R \frac{d\hat{\Omega}}{dR} b_R + \hat{\Omega} b_R + i k R \hat{\Omega} b_z \right), \quad (25)$$

$$\hat{E}_z = \frac{i m}{R} \left( \hat{B} u_z - \text{Rm} \hat{\Omega} R b_z \right). \quad (26)$$

Here we have used the notations

$$\Omega = \Omega_{\text{in}} \hat{\Omega} \quad \text{and} \quad B_{\phi} = B_{\text{in}} \hat{B}. \quad (27)$$

The diffusion terms are

$$D_R(\mathbf{b}) = \frac{d^2 b_R}{dR^2} - \frac{m^2}{R^2} b_R - k^2 b_R + \frac{1}{R} \frac{db_R}{dR} - \frac{2im}{R^2} b_{\phi} - \frac{b_R}{R^2}, \quad (28)$$

$$D_\phi(\mathbf{b}) = \frac{d^2 b_\phi}{dR^2} - \frac{m^2}{R^2} b_\phi - k^2 b_\phi + \frac{1}{R} \frac{db_\phi}{dR} + \frac{2im}{R^2} b_R - \frac{b_\phi}{R^2} \quad (29)$$

and

$$D_z(\mathbf{b}) = \frac{d^2 b_z}{dR^2} - \frac{m^2}{R^2} b_z - k^2 b_z + \frac{1}{R} \frac{db_z}{dR}. \quad (30)$$

In the same way the normalized momentum equation can be written as

$$\text{Re} \left[ \frac{\partial \mathbf{u}}{\partial t} + (\mathbf{U} \nabla) \mathbf{u} + (\mathbf{u} \nabla) \mathbf{U} \right] = \mathbf{D}(\mathbf{u}) - \nabla P + \text{Ha}^2 (\text{curl} \mathbf{B} \times \mathbf{b} + \text{curl} \mathbf{b} \times \mathbf{B}), \quad (31)$$

so that

$$i\omega \text{Re} \mathbf{u} + \text{Re} \mathbf{G} = \mathbf{D}(\mathbf{u}) - \nabla P + \text{Ha}^2 \mathbf{L} \quad (32)$$

with

$$G_R = im \hat{\Omega} u_R - 2 \hat{\Omega} u_\phi, \quad (33)$$

$$G_\phi = (R^2 \hat{\Omega})' \frac{u_R}{R} + im \hat{\Omega} u_\phi, \quad (34)$$

$$G_z = \hat{\Omega} im u_z \quad (35)$$

and

$$L_R = + \frac{im}{R} \hat{B} b_R - 2 \frac{\hat{B}}{R} b_\phi, \quad (36)$$

$$L_\phi = \frac{1}{R} (R \hat{B})' b_R + \frac{im}{R} \hat{B} b_\phi, \quad (37)$$

$$L_z = + i \frac{m}{R} \hat{B} b_z. \quad (38)$$

The perturbed flow as well as the perturbed magnetic field are source-free, i.e.

$$\frac{du_R}{dR} + \frac{u_R}{R} + i \frac{m}{R} u_\phi + ik u_z = 0 \quad (39)$$

and

$$\frac{db_R}{dR} + \frac{b_R}{R} + i \frac{m}{R} b_\phi + ik b_z = 0. \quad (40)$$

An appropriate set of ten boundary conditions is needed to solve the system. No-slip conditions as well as zero normal components for the velocity on the walls results in

$$u_R = u_\phi = u_z = 0. \quad (41)$$

The boundary conditions for the magnetic field depend on the electrical properties of the walls. The tangential currents and the radial component of the magnetic field vanish on conducting walls hence

$$\frac{db_\phi}{dR} + \frac{b_\phi}{R} = b_R = 0. \quad (42)$$

These boundary conditions hold both for  $R = R_{\text{in}}$  and for  $R = R_{\text{out}}$ .

## 4 Results

The equations have been solved for a simple model. The normalized gap width between the cylinders is 0.5 and the rotation law is rather flat approaching  $\Omega \propto R^{-1}$  hence  $\mu_\Omega = 0.5$ . The toroidal field in the gap is almost uniform ( $\mu_B = 1$ ) but it is not current-free. This field violates (8) and is therefore Tayler-unstable with a critical Hartmann number of about 150 (Rüdiger et al. 2007b). This instability is strongly modified by the differential rotation. The results are given in the Fig. 3 for the Hall parameters  $\beta_0 = -0.01, 0$  and  $0.01$ . The Hall parameter  $\beta_0$  and the magnetic Prandtl number are the free parameters of the system. Note, however, that due to (7) only  $\sqrt{\text{Pm}}\beta_0$  is a physical parameter in the definition of the Hall quantity  $\hat{\beta}$ . As only the combination of  $\beta_0 \text{Ha}$  comes into the equations we can fix the sign of  $\beta_0$  and make the calculations for positive and negative Ha values or we can fix Ha as positive and use both signs of  $\beta_0$ . We prefer the second possibility so that the results for positive and negative  $\beta_0$  correspond to opposite magnetic field orientations.

The solid line in Fig. 3 (bottom) is identical with the marginal limit between stability and instability in Fig. 1. We find that the system is destabilized by the rotation for high magnetic Prandtl numbers ( $\text{Pm} = 100$ ). In contrast, for  $\text{Pm} = 1$  the rotation *stabilizes* the flow (Fig. 3, top), which demonstrates very clearly the significant differences between the solutions with large and small magnetic Prandtl numbers.

In all these cases, however, the Hall effect acts in the same direction. For positive  $\beta$  the stability domain is reduced and for negative  $\beta$  the stability domain is increased. The stabilization (destabilization) of negative (positive) Hall  $\beta$  is a very common phenomenon of all the models. In other words, positive  $B_\phi$  (i.e.  $\beta > 0$ ) lead to smaller critical field amplitudes than negative  $B_\phi$  (i.e.  $\beta < 0$ ). Hence, if indeed the nonaxisymmetric Tayler instability limits the strength of the induced toroidal fields  $B_\phi$  then the resulting amplitudes are different for different signs of  $B_\phi$  due to the action of the Hall effect.

### 4.1 Cell structure

The cell structure of the neutrally stable modes is represented by the resulting vertical wavenumber  $k$ . From the normalizations it follows the relation

$$\frac{\delta z}{R_{\text{out}} - R_{\text{in}}} = \frac{\pi}{k} \sqrt{\frac{\hat{\eta}}{1 - \hat{\eta}}} \quad (43)$$

for the vertical cell size in units of the gap width so that for  $\hat{\eta} = 0.5$

$$\frac{\delta z}{R_{\text{out}} - R_{\text{in}}} = \frac{\pi}{k}. \quad (44)$$

Hence, for  $k \simeq \pi$  the cells are spherical while for  $k \gg \pi$  they are rather flat. Both possibilities are realized in the calculations. In Fig. 4 the results for  $\text{Pm} = 100$  are extended to

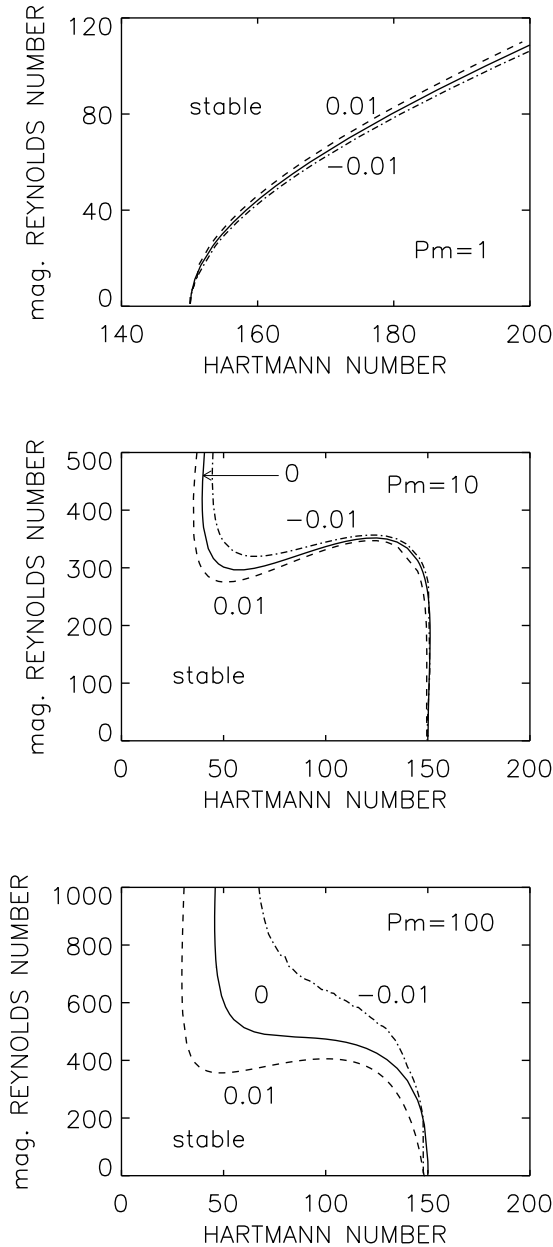


**Fig. 3** Taylor instability ( $m = 1$ ) for various magnetic Prandtl numbers  $Pm$  and with Hall effect.  $\mu_B = 1$ ,  $\mu_\Omega = 0.5$ . The curves are labeled by the Hall parameter  $\beta_0$ . Note that positive  $\beta$  reduces the stability domain while negative  $\beta$  increases it.

much higher values of the magnetic Reynolds number. The difference of the stability domains for different Hall parameters grows even bigger as the rotation increases. The curves are marked with the corresponding wave number values. We find that for negative  $\beta$  the cells are spherical but they are rather flat for positive  $\beta$ . Thus, not only the stability domains strongly differ for the Taylor instability for opposite signs of the Hall parameter but also the shape of the nonax-

isymmetric Taylor vortices depends on that sign. If indeed realized in nature then the *sign of the toroidal magnetic field* (in relation to the rotation axis) can easily be read from the observations.

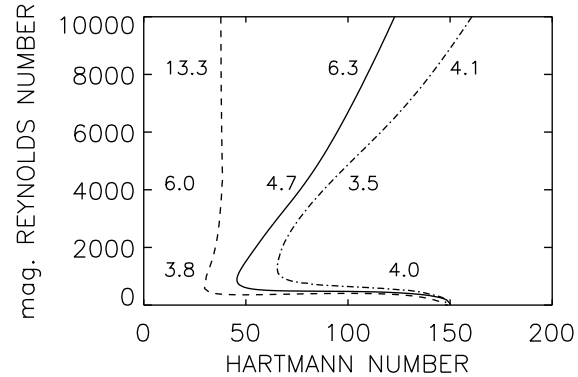


**Fig. 4** The same as in Fig. 3 (bottom,  $Pm = 100$ ). Stability only exists at left from the curves. They are marked with the wavenumbers of the marginal instability. The numbers show that also the cell structure strongly depends on the sign of the Hall effect.

## 5 Growth rates

As the Hall time is much longer than the rotation time the question arises whether the Hall effect strongly enhances the growth times of the Taylor instability. However, for the considered parameters the Hall effect hardly influences the growth rates of the Taylor instability (Fig. 5). Nevertheless, the Hall effect plays an important role for the stability map of the Taylor instability but not in the resulting linear growth rates of the unstable disturbances. The growth rates are computed along vertical lines at  $Ha = 100$  and  $Ha = 140$  in Fig. 4. The curves are marked with the Hall parameter  $\beta_0$  also including  $\beta = 0$ . The growth rates are given in units of the angular velocity of the inner cylinder, at the stability lines they vanish. A growth rate of 0.01 means an e-folding time of the instability of about 16 rotation periods. For  $Pm = 100$  this is the characteristic value for the Taylor instability without Hall effect. This time is decreased by positive Hall effect and it is increased by negative Hall effect. For positive Hall effect the Taylor instability results as much faster than the Taylor instability for negative Hall effect. All the growth rates grow with growing Hartmann numbers.

Even a weak Hall effect does not generally prolong the growth time of the Taylor instability which scales with the rotation time. In this case the Hall effect is only a modification of another instability. Even if the Hall effect itself forms the instability (together with the differential rotation)

also then the ('shear-Hall') instability scales with the rotation rate and not with the rather long Hall time (Rüdiger & Kitchatinov 2005).

Another example for this phenomenon is given by the plane-wave solution of an  $\alpha - \Omega$  dynamo. Both growth rate and cycle time of the most unstable mode of a linear oscillating  $\alpha\Omega$  dynamo with weak  $\alpha$ -effect are mainly fixed by the basic rotation:  $\gamma/\Omega \propto (\omega_\eta/\Omega)^{1/3}$ . Here  $\gamma$  is the growth rate,  $\omega_\eta$  the dissipation frequency and  $\Omega$  the basic rotation.

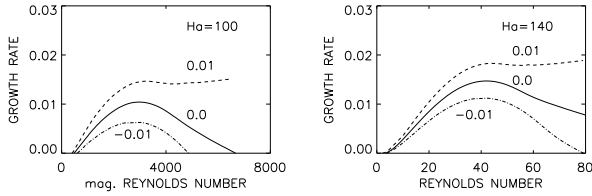


**Fig. 5** The growth rates of the Tayler instability normalized with  $\Omega_{\text{in}}$  for  $m = 1$  with and without Hall effect. The curves are marked by their Hall parameter  $\beta_0$ . The values belong to a vertical line for  $\text{Ha} = 100$  (left) and  $\text{Ha} = 140$  (right) in Fig. 4.  $\text{Pm} = 100$ ,  $\mu_B = 1$ ,  $\mu_\Omega = 0.5$ .

## 6 Steeper magnetic profile

The radial profile of the toroidal magnetic field used in Fig. 3 is rather smooth. Without detailed simulations one cannot not know the real profile. Hence, the computations represented in Fig 3 are thus repeated for different magnetic field profiles for the most interesting case of high magnetic Prandtl number ( $\text{Pm} = 100$ ).

Figure 6 has been obtained for magnetic fields that increase outwards ( $\mu_B = 3$ ). According to the Tayler criterion (8) such profiles are highly destabilizing. Consequently, we find the critical Hartmann number for  $\text{Re} = 0$  one order of magnitude smaller than in Fig. 3. The opening of the two curves for  $\beta = \pm 0.01$  is with about factor 2 for  $\text{Rm} \simeq 1000$  very similar to the previous case. Again, generally the stability domain for positive  $\beta$  is much smaller than for negative  $\beta$ . These basic findings do not depend on the actual Hartmann numbers for various magnetic profiles. Nevertheless, we should underline that with the given parameters ( $\rho \simeq 10^{13} \text{g/cm}^3$ ,  $\nu \simeq 10^9 \text{cm}^2/\text{s}$ ,  $\eta \simeq 10^7 \text{cm}^2/\text{s}$ ) for  $\text{Ha} \simeq 100$  the maximal stable magnetic field is  $3 \times 10^{12} \text{G}$  which value even grows for thinner layers.

## 7 Asymmetry of the neutron star hemispheres

Wardle (1999) has shown that due to the Hall effect the stability properties of a differentially rotating MHD flow depend on the sign of the axial magnetic field. After our results the same is true for the azimuthal magnetic field. Moreover,

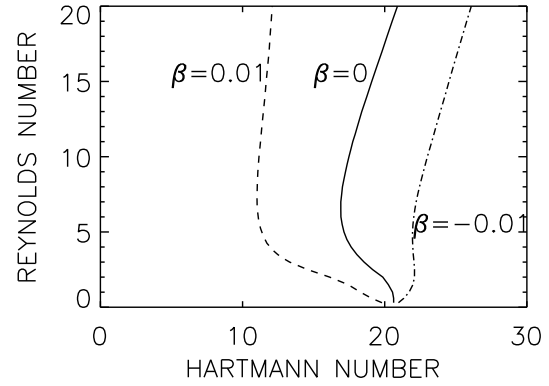


**Fig. 6** Taylor instability ( $m = 1$ ) for steep magnetic field ( $\mu_B = 3$ ), for large magnetic Prandtl number ( $\text{Pm} = 100$ ) and with Hall effect.  $\mu_\Omega = 0.5$ . The curves are labeled by their Hall parameter  $\beta_0$ .

the critical magnetic field value above which the flow becomes unstable can basically differ for different magnetic field orientations (Fig. 3, bottom).

If the effect is strong enough this finding can have consequences. If in a PNS with differential rotation the toroidal field results from a poloidal field with dipolar symmetry then also the  $B_\phi$  is antisymmetric with respect to the equator. If the Tayler instability indeed determines the maximal field amplitudes then due to the Hall effect the amplitudes of the toroidal field in both hemispheres become different. Obviously, the Tayler-Hall instability produces an extra quadrupolar component of the originally produced toroidal fields with dipolar symmetry. It is thus unavoidable that the amplitudes of the induced toroidal field belts are different in both hemispheres.

For  $\text{Ha} \sim 100$ ,  $\text{Pm} \sim 100$  and  $\beta_0 \sim 10^{-2}$  taken from the bottom plot of Fig. 3 we find for the Hall parameter  $\hat{\beta} \sim 10$  leading to  $\sim 10^{13} \text{G}$  for the neutron star. This value is typical for pulsars so that the conclusion about different toroidal field values in both the hemispheres of a neutron star due to Tayler-Hall effects becomes realistic.

On the other hand, strong magnetic fields suppress the heat transport in neutron stars (Schaaf 1988, 1990; Heyl & Hernquist 1998). The heat transport is blocked in the direction perpendicular to the field lines so that the heat conductivity tensor becomes anisotropic, i.e.

$$\chi_{ij} = \chi_1 \delta_{ij} + \chi_2 B_i B_j, \quad (45)$$

where  $\chi_1$  represents the heat flux perpendicular to the field which is quenched by strong magnetic fields, hence (say)  $\chi_1 \propto 1/(1 + \hat{\beta}^2)$ . With

$$\chi_{ij} = \frac{\chi_0}{1 + \hat{\beta}^2} \left( \delta_{ij} + \hat{\beta}^2 \frac{B_i B_j}{B^2} \right) \quad (46)$$

the heat flux remains finite along the field lines even for  $B \rightarrow \infty$ .

The consequence of this magnetic-induced anisotropy of the heat flux tensor is a global inhomogeneity of the surface temperature (Geppert et al. 2006). If the latitudinal distribution of the magnetic field is strictly symmetric or anti-symmetric with respect to the equator then the surface temperature results as equator-symmetric. This is not true if for both hemispheres the magnetic amplitudes are differing (or, in other words, if the total magnetic field is a combination of a dipole and a quadrupole). Exactly this is the case if the toroidal magnetic field is produced by differential rotation under the presence of Tayler-Hall instability. If the differential rotation of the neutron star disappears then the magnetic fields are frozen in so that the magnetic constellation is conserved for the time scales of the Ohmic decay (also modified by the Hall effect). We do thus expect the two half spheres of an isolated neutron star to be of different X-ray activity.

Schwope et al. (2005) have indeed found an equatorial-asymmetric X-ray brightness analyzing XMM observations of the isolated neutron star RBS1223. The authors have assumed the existence of one bright “spot” in each of the hemispheres and found two temperature maxima of different strength (ratio  $\epsilon = 0.91$ ). If this asymmetry effect is general for neutron stars then the interior magnetic fields must also be asymmetric with respect to the equator (dipole plus quadrupole) which can be explained with the Tayler-Hall scenario with differential rotation developed in the present paper.

*Acknowledgements.* D.A.S. acknowledges the financial support from the Deutsche Forschungsgemeinschaft. The simulations were performed with the computer cluster SANSSOUCI of the AIP.

## References

- Andersson, N.: 1998, ApJ 502, 708  
 Ardeljan, N.V., Bisnovaty-Kogan, G.S., Moiseenko, S.G.: 2005, MNRAS 359, 333  
 Bonanno, A., Rezzolla, L., Urpin, V.A.: 2003, A&A 410, L33  
 Bonanno, A., Urpin, V.A., Belvedere, G.: 2006, A&A 451, 1049  
 Burrows, A.: 1987, ApJ 318, L57  
 Burrows, A., Dessart, L., Livne, E., Ott, C.D., Murphy, J.: 2007, ApJ 664, 416  
 Cumming, A., Arras, P., Zweibel, E.: 2004, ApJ 609, 999  
 Dimmelmeyer, H., Font, J.A., Müller, E.: 2002, A&A 393, 523  
 Friedman, J.L., Schutz, B.F.: 1978, ApJ 222, 281  
 Geppert, U., Küker, M., Page, D.: 2006, A&A 457, 937  
 Goldreich, P., Reisenegger, A.: 1992, ApJ 395, 250  
 Heyl, J.S., Hernquist, L.: 1998, MNRAS 300, 599  
 Jones, P.B.: 1988, MNRAS 233, 875  
 Kotake, K., Sawai, H., Yamada, S., Sato, K.: 2004, ApJ 608, 391  
 Lindblom, L., Tohline, J.E., Vallisneri, M.: 2001, Phys Rev Lett 86, 1152  
 Naso, L., Rezzolla, L., Bonanno, A., Paternó, L.: 2007, arXiv:0711.1498  
 Ott, C.D., Ou, S., Tohline, J.E., Burrows, A.: 2005, A&A 625, L119  
 Potekhin, A.Y.: 1999, A&A 351, 787  
 Rezzolla, L., Lamb, F.K., Shapiro, S.L.: 2000, ApJ 531, L139  
 Rüdiger, G., Kitchatinov, L.L.: 2005, A&A 434, 629  
 Rüdiger, G., Hollerbach, R., Schultz, M., Elstner, D.: 2007a, MNRAS 377, 1481  
 Rüdiger, G., Schultz, M., Shalybkov D.A., Hollerbach, R.: 2007b, Phys Rev E 76, 056309  
 Schaaf, M.E.: 1988, A&A 205, 335  
 Schaaf, M.E.: 1990, A&A 235, 499  
 Schwope, A., Hambaryan, V., Haberl, F., Motch, C.: 2005, A&A 441, 597  
 Shalybkov, D.A., Urpin, V.A.: 1995, MNRAS 273, 643  
 Shapiro, S.L.: 2000, ApJ 544, 397  
 Stergioulas, N., Font, J.A.: 2001, Phys Rev Lett 86, 1148  
 Tayler, R.J.: 1961, JNuE C 5, 345  
 Tayler, R.J.: 1973, MNRAS 161, 365  
 Thompson, C., Duncan, R.C.: 1993, ApJ 408, 194  
 Urpin, V.A., Rüdiger, G.: 2005, A&A 437, 23  
 Vandakurov, Y.V.: 1972, SvA 16, 265  
 Wardle, M.: 1999, MNRAS 307, 849  
 Watts, A.L., Andersson, N.: 2002, MNRAS 333, 943  
 Yakovlev, D.G., Shalybkov, D.A.: 1991, Ap&SS 176, 171  
 Yakovlev, D.G., Shalybkov, D.A.: 1991, Ap&SS 176, 191